

Hidden exceptional point, localization-delocalization phase transition in Hermitian bosonic Kitaev model

D. K. He and Z. Song*

School of Physics, Nankai University, Tianjin 300071, China

Exceptional points (EPs), a unique feature of non-Hermitian systems, represent degeneracies in non-Hermitian operators that likely do not occur in Hermitian systems. Nevertheless, unlike its fermionic counterpart, a Hermitian bosonic Kitaev model supports a non-Hermitian core matrix, involving a quantum phase transition (QPT) when an exceptional point appears. In this study, we examine QPTs by mapping the Hamiltonian onto a set of equivalent single-particle systems using a Bardeen-Cooper-Schrieffer (BCS)-like pairing basis. We demonstrate the connection between the hidden EP and the localization-delocalization transition in the equivalent systems. The result is applicable to a Dicke model, which allows the experimental detection of the transition based on the measurement of the average number of photons for the quench dynamics starting from the empty state. Numerical simulations of the time evolution reveal a clear transition point at the EP.

I. INTRODUCTION

An exclusive feature of non-Hermitian systems is the concept of exceptional points (EPs) [1–3], which are the degeneracies of non-Hermitian operators. The dynamics of the system with parameters far away from, near and at the EP, exhibits extremely different behaviors [4–6]. Consider a 2×2 non-Hermitian matrix as an illustrative example. The matrix has two identical eigenvectors at the EP. (i) When the system is far from or near an EP and has a finite energy gap ϵ , the dynamics exhibit periodic oscillations, with the associated Dirac probability oscillating over a period of $2\pi/\epsilon$. (ii) When the system is at an EP, the Dirac probability increases quadratically with time. (iii) When the system has complex energy levels, the Dirac probability increases exponentially with time. The distinctive characteristics surrounding the EP have ignited significant interest in both classical and quantum photonic systems [7–13].

A question that may seem naive but is actually insightful is whether there is an EP hidden within a Hermitian system. The previous works [14–17] for non-interacting systems indicates that there exists a connection between the EPs of an effective non-Hermitian system on a finite lattice and the dynamic behavior in a finite-size Hermitian system. It is referred to as EP dynamics, which stands for the exclusive dynamic behaviors and properties of a non-Hermitian system at EP. This motivates us to reveal the connection between the EP and the dynamics for an interacting many-body system.

Recently, the study of the bosonic Kitaev model has received much attention [18–27]. In contrast to its fermionic counterpart, the Hermitian bosonic Kitaev model features a non-Hermitian core matrix within its Nambu representation. It appears that the EP is not a unique feature of non-Hermitian systems. Although such a non-Hermitian matrix cannot result in a complex quasi-particle spectrum of the original Hermitian Hamiltonian,

special dynamic behaviors may be associated with the emergence of its EP. It is our goal to establish the connection between hidden EP and the possible phase transition in dynamic behaviors of the system.

In this work, we examine the QPTs that arise from the EPs in a Hermitian bosonic Kitaev model by exploring the exact solutions. It is demonstrated that an EP exists in the core matrix with a given momentum, which results in a non-analytic point in the solutions. We map the Hamiltonian onto a set of equivalent single-particle systems using a Bardeen-Cooper-Schrieffer (BCS)-like pairing basis. We demonstrate the connection between the hidden EP and the localization-delocalization transition in the equivalent systems. In addition, we apply the result to a Dicke model, which allows the experimental detection of the transition based on the measurement of the average photon number for the time evolution of the initial empty state.

Our results provide an alternative approach for bosonic Kitaev models. The structure of this paper is as follows. In Sec. II, we introduce the model and present the phase diagram in Sec. III. In Sec. IV, we investigate the localization-delocalization transition in the Fock space. In Sec. V, we delve into the EP-associated transition within the Dicke model, focusing on the quenching dynamics. Finally, in Sec. VI, we provide a summary and discussion.

II. MODEL

The fermionic Kitaev chain is a one-dimensional tight-binding model with the nearest-neighbor hopping and the superconducting p -wave pairing terms on each dimer [28]. The corresponding bosonic Kitaev model on N lattice with imaginary hopping and pairing amplitudes can be written as

$$H = \sum_{j=1}^N [itb_{j+1}^\dagger b_j + i\Delta b_{j+1}^\dagger b_j^\dagger + \text{H.c.} + \mu (2b_j^\dagger b_j + 1)], \quad (1)$$

* songtc@nankai.edu.cn

where b_j^\dagger (b_j) is a bosonic creating (annihilation) operator on site j . The periodic boundary condition is imposed by defining $b_1 = b_{N+1}$. Here, the hopping strength t and chemical potential μ are always real in this work. In this work, we only consider the case with $\mu > 0$ and real Δ for the sake of simplicity. Using the Fourier transformation

$$b_j = \frac{1}{\sqrt{N}} \sum_{-\pi \leq k < \pi} e^{ikj} b_k. \quad (2)$$

we get the Hamiltonian in k -space in the form

$$H = 2 \sum_{0 \leq k < \pi} [(\mu + t \sin k) b_k^\dagger b_k + (\mu - t \sin k) b_{-k} b_{-k}^\dagger + i\Delta \cos k b_k^\dagger b_{-k}^\dagger + \text{H.c.}]. \quad (3)$$

In order to get the solution of the Hamiltonian, we rewrite it in the block diagonal form $H = \sum_{0 \leq k < \pi} H_k$, satisfying the commutation relation $[H_k, H_{k'}] = 0$. It differs slightly from the fermionic Kitaev model in that the Nambu representation of H_k equals

$$H_k = 2 \begin{pmatrix} b_k^\dagger & -b_{-k} \end{pmatrix} h_k \begin{pmatrix} b_k \\ b_{-k}^\dagger \end{pmatrix}, \quad (4)$$

where the core matrix h_k is [18]

$$h_k = \begin{pmatrix} \mu & i\Delta_k \\ i\Delta_k & -\mu \end{pmatrix} + T_k, \quad (5)$$

with $T_k = t \sin k$ and $\Delta_k = \Delta \cos k$. We observed that the matrix h_k is non-Hermitian and becomes a Jordan block

$$h_k^{\text{JD}} = \mu \begin{pmatrix} 1 & i \\ i & -1 \end{pmatrix} + T_k, \quad (6)$$

satisfying $(h_k^{\text{JD}} - T_k)^2 = 0$, when taking $\mu = \Delta_k$, which is referred to as EP of the matrix. h_k^{JD} is not diagonalizable and possesses a coalescing eigenvector $(-i, 1)$. It is evident that the Hermiticity of h_k within the Hermitian Hamiltonian H does not preclude the possibility of non-Hermitian dynamics. Therefore, the existence of EP for the non-Hermitian matrix h_k should affect the property of the solutions, resulting a sudden change of the corresponding dynamics of H . The main goal of this work is to explore the connection between the EP of h_k and the transition point of the dynamics.

III. PHASE DIAGRAM

Let us firstly determine the phase diagram by studying the eigen problem of the matrix h_k . For the case with $\mu^2 \neq \Delta_k^2$, taking a similarity transformation

$$V_k = \begin{pmatrix} -i \sinh \frac{\theta_k}{2} & \cosh \frac{\theta_k}{2} \\ \cosh \frac{\theta_k}{2} & i \sinh \frac{\theta_k}{2} \end{pmatrix}, \quad (7)$$

the matrix h_k can be diagonalized as

$$(V^k)^{-1} h_k V^k = \begin{pmatrix} \varepsilon_+^k & 0 \\ 0 & \varepsilon_-^k \end{pmatrix} + T_k, \quad (8)$$

with the eigenvalue

$$\varepsilon_\pm^k = \pm 2\sqrt{\mu^2 - \Delta_k^2}. \quad (9)$$

Here the parameter θ_k is determined by

$$\tanh \frac{\theta_k}{2} = \frac{\mu - \varepsilon_+^k}{\Delta_k}, \quad (10)$$

which can be complex. Based on the results, the Hamiltonian can be written as the form

$$H = 2 \sum_{-\pi \leq k < \pi} [(\varepsilon_+^k - T_k) \left(\bar{\gamma}_k \gamma_k + \frac{1}{2} \right)], \quad (11)$$

where the complex Bogoliubov modes defined as

$$\begin{aligned} \gamma_k &= i \sinh \frac{\theta_k}{2} b_k^\dagger + \cosh \frac{\theta_k}{2} b_{-k}, \\ \bar{\gamma}_k &= -i \sinh \frac{\theta_k}{2} b_k + \cosh \frac{\theta_k}{2} b_{-k}^\dagger, \end{aligned} \quad (12)$$

and

$$\begin{aligned} \gamma_{-k} &= i \sinh \frac{\theta_k}{2} b_{-k}^\dagger + \cosh \frac{\theta_k}{2} b_k, \\ \bar{\gamma}_{-k} &= -i \sinh \frac{\theta_k}{2} b_{-k} + \cosh \frac{\theta_k}{2} b_k^\dagger, \end{aligned} \quad (13)$$

satisfying the canonical relations

$$\begin{aligned} [\gamma_k, \bar{\gamma}_{k'}] &= \delta_{kk'}, \\ [\gamma_k, \gamma_{k'}] &= [\bar{\gamma}_k, \bar{\gamma}_{k'}] = 0, \end{aligned} \quad (14)$$

with $k \in (-\pi, \pi]$.

It appears that the Hamiltonian H in Eq. (11) is in diagonal form. However, an additional necessary condition for diagonalization is the existence of a vacuum state $|\text{Vac}\rangle$ for the operator γ_k , such that $\gamma_k |\text{Vac}\rangle = 0$. When the vacuum state of the operator γ_k is given, all the eigenstates can be constructed. In situations where the explicit expression of the vacuum state is not available, one can investigate the existence of such a state in the following manner. (i) In the case where $\mu > |\Delta_k|$, direct derivation shows that θ_k is real for any k , which results in $\bar{\gamma}_k = \gamma_k^\dagger$. Subsequently, the Hamiltonian H can be expressed in the diagonal form

$$H = 2 \sum_{-\pi \leq k < \pi} [(\varepsilon_+^k - T_k) \left(\hat{\mathcal{N}}_k + \frac{1}{2} \right)]. \quad (15)$$

where $\hat{\mathcal{N}}_k = \gamma_k^\dagger \gamma_k$ is the quasi-boson number operator. If the vacuum state $|\text{Vac}\rangle$ exists, the energy levels are

$$E_k = 2(\varepsilon_+^k - T_k) \left(\mathcal{N}_k + \frac{1}{2} \right), \quad (16)$$

where integers $\mathcal{N}_k \in [0, \infty]$, and $k \in (-\pi, \pi]$. Notably, the energy levels are equidistant with level spacing $\varepsilon_+^k + T_k$ for fixed k . These results are self-consistent with the fact that the Hamiltonian H is Hermitian. (ii) In contrast, in the case where $\mu < |\Delta_k|$, we note that ε_+^k is imaginary. If the vacuum state $|\text{Vac}\rangle$ exists, it is also the eigenstate of H , that is,

$$H|\text{Vac}\rangle = i \sum_{-\pi \leq k < \pi} |\varepsilon_+^k| |\text{Vac}\rangle. \quad (17)$$

Obviously, the presence of imaginary parts in the eigenvalues is self-consistent with the fact that the Hamiltonian H is Hermitian. It implies that the vacuum state $|\text{Vac}\rangle$ does not exist, and the corresponding Bogoliubov transformation is not the proper method for diagonalization when $\mu < |\Delta_k|$.

This analysis predicts that the existence of EP for the core matrix h_k will be reflected in the eigenstates and dynamics of the system. In the following section, we will demonstrate and verify this point from an alternative perspective.

IV. LOCALIZATION-DELOCALIZATION TRANSITION

In this section, we investigate the Hamiltonian H in Eq. (1) based on its equivalent Hamiltonian, which describes the same physical system under a different representation. We map the Hamiltonian onto a set of single-particle systems using a Bardeen-Cooper-Schrieffer (BCS)-like pairing basis. We demonstrate the connection between the EP and the localization-delocalization transition in the equivalent systems.

There are many invariant subspaces for H_k arising from the symmetries

$$[\Pi, H_k] = [K, H_k] = 0, \quad (18)$$

where two operators are the boson number parity operator

$$\Pi = (-1)^{n_k + n_{-k}}, \quad (19)$$

and total momentum operator

$$K = k(n_k - n_{-k}), \quad (20)$$

with $n_k = b_k^\dagger b_k$. Here, we consider the case of a simply invariant subspace, which is spanned by a basis set $\{|l\rangle, l \in [0, \infty)\}$

$$|l\rangle = \frac{1}{l!} \left(b_k^\dagger b_{-k}^\dagger \right)^l |0\rangle_k |0\rangle_{-k} \quad (21)$$

with $\Pi|l\rangle = |l\rangle$ and $K|l\rangle = 0|l\rangle$, where $|0\rangle_k$ is the vacuum state for boson operator b_k , i.e., $b_k|0\rangle_k = 0$. Based on

this set of basis, the equivalent Hamiltonian of H_k can be expressed as the form

$$H_{\text{eq}}^k = i2\Delta_k \sum_{l=0}^{\infty} [((l+1)|l+1\rangle\langle l| - \text{H.c.}) + 2\mu l|l\rangle\langle l|], \quad (22)$$

which describes a single-particle chain with an l -dependent nearest-neighbor (NN) hopping term and linear potential. We still consider the solutions of the equivalent Hamiltonian in the two regions, separated by the EP.

(i) In the case where $\mu > |\Delta_k|$, a straightforward derivation shows that the state

$$|\text{Vac}\rangle = \sum_{l=0}^{\infty} (i)^{l+1} \left(-\frac{E_{\text{Vac}}^k}{2\Delta_k} \right)^l |l\rangle, \quad (23)$$

is the eigenstate of H_{eq}^k , satisfying $H_{\text{eq}}^k |\text{Vac}\rangle = E_{\text{Vac}}^k |\text{Vac}\rangle$ with energy

$$E_{\text{Vac}}^k = 2\sqrt{\mu^2 - \Delta_k^2} - 2\mu, \quad (24)$$

under the condition $\mu^2 \geq \Delta_k^2$. Importantly, it is just the vacuum state of the operator γ_k , i.e.,

$$\gamma_k |\text{Vac}\rangle = 0, \quad (25)$$

based on which, other eigenstates of H_{eq}^k can be constructed as $(\gamma_k^\dagger \gamma_{-k}^\dagger)^n |\text{Vac}\rangle$ for integer n , with energy

$$E_n^k = 4n\sqrt{\mu^2 - \Delta_k^2} - 2\mu. \quad (26)$$

The profile of the wave function of $|\text{Vac}\rangle$ is plotted in Fig. 1(a). It indicates that state $|\text{Vac}\rangle$ is a localized state.

(ii) In the case where $\mu < |\Delta_k|$, the above solution is invalid, and we must then seek another way. To proceed, we introduce another boson operator

$$\bar{b}_k = i\kappa_+ b_k^\dagger + \kappa_- b_{-k}, \quad (27)$$

with

$$\kappa_{\pm} = \frac{\sqrt{|\Delta_k| - \mu} \mp \sqrt{|\Delta_k| + \mu}}{2(\Delta_k^2 - \mu^2)^{1/4}}, \quad (28)$$

to rewrite H^k in the form

$$H_k = i\sqrt{\Delta_k^2 - \mu^2} \left(\bar{b}_{-k}^\dagger \bar{b}_k^\dagger - \bar{b}_k \bar{b}_{-k} \right) + T_k \left(\bar{b}_{-k}^\dagger \bar{b}_{-k} - \bar{b}_k^\dagger \bar{b}_k \right) - \mu. \quad (29)$$

Similarly, we consider the case of a simply invariant subspace, which is spanned by a basis set $\{|\bar{l}\rangle, l \in [0, \infty)\}$

$$|\bar{l}\rangle = \frac{1}{l!} \left(\bar{b}_k^\dagger \bar{b}_{-k}^\dagger \right)^l |\bar{0}\rangle_k |\bar{0}\rangle_{-k}, \quad (30)$$

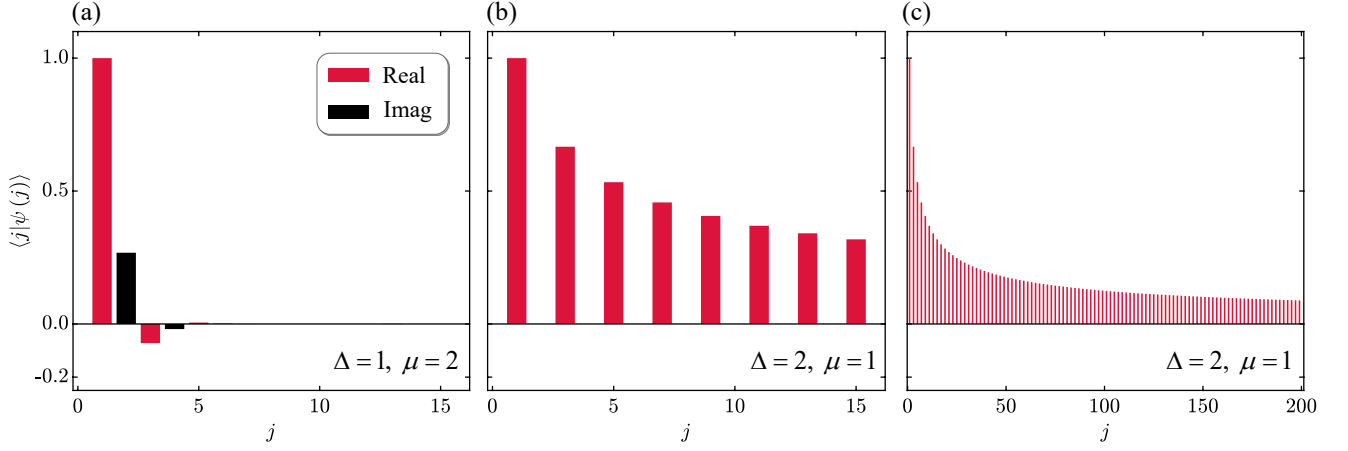


FIG. 1. Plots of two eigenstates $|\psi\rangle$ of the equivalent Hamiltonian H_{eq}^k , given by Eq. (22), with two typical system parameters (a) $\Delta_k = 1$ and $\mu = 2$, and (b, c) $\Delta_k = 2$ and $\mu = 1$, respectively. Here, the red or black bars represent the real or imaginary parts of the amplitudes, respectively, and all are analytically determined. (a) The profile of the vacuum state ($|\psi\rangle = |\text{Vac}\rangle$) is obtained from Eq. (23), which is also the ground state with energy $E_{\text{vac}}^k = -0.5359$. It decays exponentially and then a localized state. (b, c) is the profile of the eigenstate ($|\psi\rangle = |\varphi_k\rangle$) with energy $E_k = 0.0$, which is obtained from Eq. (35). (b) is the plot on the same scale as (a) for comparison, while (c) is the same plot but on longer scale. We can see from (c) that it becomes to a constant for large j , indicating a delocalized state. These results imply that the EP at $\Delta_k = \mu$ is a transition point from localization to delocalization in the Fock space.

where $|0\rangle_k$ is the vacuum state for boson operator \bar{b}_k , i.e., $\bar{b}_k|0\rangle_k = 0$. Based on this set of basis, the equivalent Hamiltonian of H_k can be expressed as the form

$$\begin{aligned} \bar{H}_{\text{eq}}^k &= i2\sqrt{\Delta_k^2 - \mu^2} \sum_{l=0}^{\infty} ((l+1) \overline{|l+1\rangle} \langle l| \\ &\quad - \text{H.c.}) - \mu, \end{aligned} \quad (31)$$

which describes a single-particle chain with an l -dependent nearest-neighbor (NN) hopping term and zero linear potential. The corresponding Schrodinger equation is

$$\bar{H}_{\text{eq}}^k |\varphi_k\rangle = E_k |\varphi_k\rangle. \quad (32)$$

The solution to such a semi-infinite chain can be exactly obtained as follows. For any given real number E_k as the eigenvalues, the corresponding eigenvector

$$|\varphi_k\rangle = \sum_{l=0}^{\infty} c_l \overline{|l\rangle}, \quad (33)$$

is given by the following recursive formula

$$\begin{aligned} c_0 &= 1, \\ c_1 &= i \frac{E_k}{\sqrt{\Delta_k^2 - \mu^2}}, \\ &\dots, \\ c_{l+1} &= \frac{l\sqrt{\Delta_k^2 - \mu^2}c_{l-1} + iE_k c_l}{(l+1)\sqrt{\Delta_k^2 - \mu^2}} \\ &\dots \end{aligned} \quad (34)$$

Taking $E_k = 0$, as an example, we have

$$\begin{aligned} c_0 &= 1, c_1 = 0, \\ c_2 &= \frac{1}{2}, c_3 = 0, \\ &\dots, \\ c_{2n} &= \frac{(2n-1)}{2n} c_{2(n-1)}, c_{2n-1} = 0 \\ &\dots, \end{aligned} \quad (35)$$

which is plotted in Fig. 1(b). The profile of the wave function indicates that the corresponding eigen state is an extended state in the space spanned by the basis set $\{\overline{|l\rangle}\}$. Although there is no rigorous proof, the following relation

$$\begin{aligned} &\langle l | (\bar{b}_k^\dagger \bar{b}_{-k}^\dagger - \bar{b}_k \bar{b}_{-k}) | l' \rangle \\ &= (\kappa_+^2 + \kappa_-^2) (l\delta_{l,l'-1} - l'\delta_{l,l'+1}) - i4\kappa_- \kappa_+ l\delta_{l,l'} \end{aligned} \quad (36)$$

implies that an extended state in the space $\{\overline{|l\rangle}\}$ is also an extended state in the space $\{|l\rangle\}$.

The above analysis implies that the eigenstates of H_{eq}^k are localized in one region ($\mu > |\Delta_k|$) and extended in the other ($\mu < |\Delta_k|$). A natural question arises: whether it is a universal conclusion for other eigenstates. At this stage, we can only answer this question with the aid of numerical simulations. To characterize the localization features, we use the inverse participation ratio (IPR) of a given state $|\psi\rangle$ as a criterion to distinguish the extended states from the localized ones. The IPR is defined as

$$\text{IPR} = \frac{\sum_l |\langle \psi | l \rangle|^4}{(\sum_l |\langle \psi | l \rangle|^2)^2}. \quad (37)$$

For spatially extended states, the value of IPR approaches zero as the system size becomes sufficiently large, whereas it remains finite for localized states, regardless of the system size. For example, the IPR for the state $|\text{Vac}\rangle$ given in Eq. (23) can be estimated as

$$\text{IPR}_V = \frac{\Delta_k^2}{\mu^2 - \mu\sqrt{\mu^2 - (\Delta_k)^2}} - 1, \quad (38)$$

which is finite, identifying it as a local state. We perform numerical simulation to explore localization-delocalization transition for a truncated chain with length L . We compute the mean inverse participation ratio (MIPR), which is the arithmetic mean of the IPRs for all the eigenstates. The finite size effect can be excluded in our analysis because the system size is large enough to approximate an infinite system. The MIPR is plotted as a function of the system parameter in Fig. 2, showing an evident sudden change at the EP.

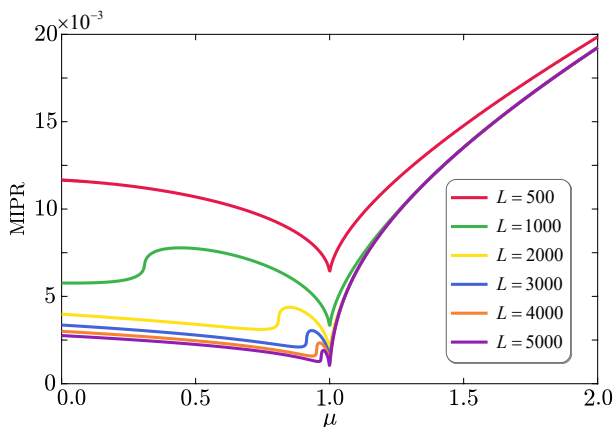


FIG. 2. Plot of MIPR, which represents the arithmetic mean of the IPRs for a set of eigenstates of the Hamiltonian H_{eq}^k , given by Eq. (22). The system parameters are $\Delta = 1$ and N indicated in the panel. The selected set of states consists of the lowest 400 eigenstates. It is evident that there is a transition point at $\mu = 1$ for every given N . Furthermore, the value of MIPR becomes stable as N increases. For $\mu < 1$, the asymptotic value of MIPR approaches zero as the system size becomes sufficiently large, whereas it remains finite for $\mu > 1$.

We would like to point out that the localization-delocalization transition occurs in the Fock space and in some invariant subspaces. This is slightly different from the usual transition in real space for systems such as the AA model and the Anderson model, where the transition is entirely determined by the system parameters.

V. QUENCH DYNAMICS IN DICKE MODEL

In this section, we utilize the results derived in the previous sections to construct a scheme for experimentally demonstrating the dynamic signature of the EP in the

Dicke model. It is a fundamental model of quantum optics, which describes the interaction between light and matter. In the Dicke model, the light component is described as a single quantum mode, while the matter is described as a set of two-level systems. The model is characterized by the following Hamiltonian for N atoms

$$H_D = \mu (a^\dagger a + J_z) + \frac{\Delta}{\sqrt{N_{\text{atom}}}} (a^\dagger + a) (J_+ + J_-), \quad (39)$$

where a^\dagger (a) is a bosonic creating (annihilation) operator. Here $\mu > 0$ is the cavity frequency, or the chemical potential of the bosons and is also the energy difference between the states of each two-level system, $\Delta > 0$ characterizes the coupling between the two-level systems and the cavity. Here, we use some special letters (μ, Δ) for the sake of consistency across contexts. We define the macroscopic spin operators J_α ($\alpha = x, y, z$) and $J_\pm = J_x \pm iJ_y$ of spin- $N/2$ to represent the collective state of N atoms, which satisfy the spin algebra, $[J_\alpha, J_\beta] = i\varepsilon_{\alpha\beta\gamma} J_\gamma$. Introducing the Holstein-Primakoff boson representation of the collective spin operators

$$\begin{aligned} J_z &= b^\dagger b - \frac{N_{\text{atom}}}{2}, \\ J_+ &= (J_-)^\dagger = b^\dagger \sqrt{N_{\text{atom}} - b^\dagger b}, \end{aligned} \quad (40)$$

the Hamiltonian can be rewritten as the form

$$H_{\text{eff}} = \mu (a^\dagger a + b^\dagger b) + \Delta (a^\dagger + a) (b^\dagger + b), \quad (41)$$

by neglecting a constant term. It is exactly the same as the two-site bosonic Kitaev model we studied in previous sections. Taking the transform

$$d_\pm = \frac{1}{\sqrt{2}} (a \pm b), \quad (42)$$

the Hamiltonian can be expressed as

$$H_{\text{eff}} = \varphi_L \begin{pmatrix} h_{\text{eff}}^+ & 0 \\ 0 & h_{\text{eff}}^- \end{pmatrix} \varphi_R, \quad (43)$$

with the non-Hermitian matrices

$$h_{\text{eff}}^\pm = \frac{\mu}{2} \begin{pmatrix} 1 & 0 \\ 0 & -1 \end{pmatrix} \pm \frac{\Delta}{2} \begin{pmatrix} 1 & 1 \\ -1 & -1 \end{pmatrix} \quad (44)$$

$$= \frac{(\mu \pm \Delta)}{2} \sigma_z \pm \frac{i\Delta}{2} \sigma_y, \quad (45)$$

where σ_z and σ_y are Pauli matrices, and the two operator vectors are $\varphi_L = (d_+, -d_+^\dagger, d_-, -d_-^\dagger)$ and $\varphi_R = (d_+^\dagger, d_+, d_-^\dagger, d_-)$. Obviously, the EP occurs at $\mu = \mu_c = \Delta$, at which one of the two matrices h_{eff}^+ and h_{eff}^- is undiagonalizable. It should result in the critical behavior both in the ground state and dynamics of H_D . In the case with $\mu \neq \Delta$, the Hamiltonian can be diagonalized as the form

$$H_{\text{eff}} = \sum_{\rho=\pm} \varepsilon_\rho \left(\bar{\gamma}_\rho \gamma_\rho + \frac{1}{2} \right), \quad (46)$$

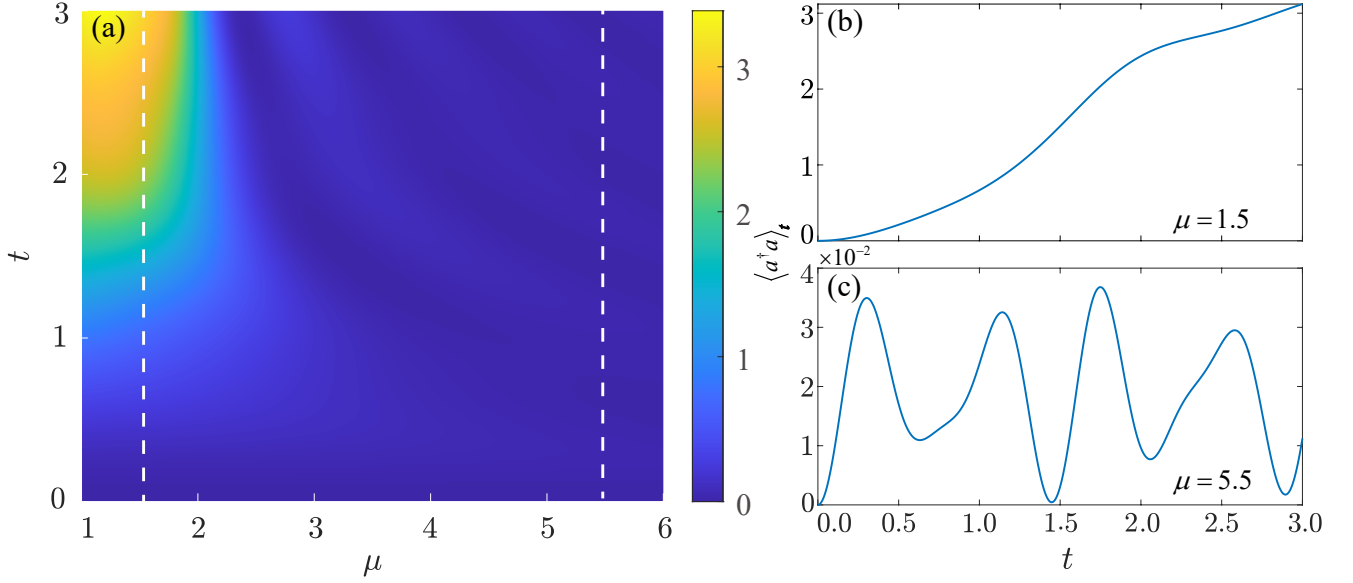


FIG. 3. Plots of the average photon number $N_P(t)$, given by Eq. (56), for the quench process in the Dicke model with the Hamiltonian H_D , as defined by the Eq. (39). The numerical simulation is performed by tracking the time evolution of the initial state $|\Psi(0)\rangle$, which is detailed in the main text preceding Eq. (56). The quantity $N_P(t)$ for a given μ is obtained by exact diagonalization of the finite-dimensional matrix representation of H_D , under the truncation of the photon number. The system parameters are an atom number $N_{\text{atom}} = 64$ and $\Delta = 1$. (a) A 3D plot of N_P as a function of time t and μ . (b, c) The profiles of $N_P(t)$ for two typical values of μ .

where the energy is

$$\varepsilon_{\sigma\rho} = \frac{\sigma}{2} \sqrt{\mu^2 + 2\rho\Delta\mu}, \quad (47)$$

and the complex Bogoliubov modes defined as

$$\begin{aligned} \gamma_\rho &= \sinh \frac{\theta_\rho}{2} d_\rho^\dagger + \cosh \frac{\theta_\rho}{2} d_\rho, \\ \bar{\gamma}_\rho &= \sinh \frac{\theta_\rho}{2} d_\rho + \cosh \frac{\theta_\rho}{2} d_\rho^\dagger, \end{aligned} \quad (48)$$

where $\tanh(\theta_\rho/2) = 1 - \rho(\mu/\Delta)(1 + \sqrt{1 + 2\rho\Delta/\mu})$, satisfying the canonical relations

$$\begin{aligned} [\gamma_\rho, \bar{\gamma}_{\rho'}] &= \delta_{\rho\rho'}, \\ [\gamma_\rho, \gamma_{\rho'}] &= [\bar{\gamma}_\rho, \bar{\gamma}_{\rho'}] = 0. \end{aligned} \quad (49)$$

As concluded before, such complex Bogoliubov modes are only available in the region $\mu > \Delta$, in which we still have $\bar{\gamma}_\pm = \gamma_\pm^\dagger$. We investigate the solutions in the two regions, respectively.

(i) In the region $\mu > \Delta$, the vacuum state of the quasi-boson operator γ_\pm is

$$|\text{Vac}_\pm\rangle = \sum_{l=0}^{\infty} (\eta_\pm)^l A_l |2l\rangle, \quad (50)$$

with $|l\rangle = \frac{1}{\sqrt{2l!}} (d_\rho^\dagger)^{2l} |0\rangle$, satisfying $\gamma_\pm |\text{Vac}_\pm\rangle = 0$, where the coefficients are given by

$$\eta_\pm = \frac{\Delta \pm \mu \mp \sqrt{\mu^2 \pm 2\Delta\mu}}{\sqrt{2}\Delta}, \quad (51)$$

and

$$\begin{aligned} A_0 &= A_1 = 1, \\ A_{l+2} &= \sqrt{\frac{2l^2 + 5l + 3}{2l^2 + 5l + 2}} \frac{(A_{l+1})^2}{A_l}. \end{aligned} \quad (52)$$

The profiles of the vacuum states

$$p_\pm(l) = \frac{|\langle 2l | \text{Vac}_\pm \rangle|^2}{\sum_{l=0} |\langle 2l | \text{Vac}_\pm \rangle|^2}, \quad (53)$$

for several representative values of μ/Δ are plotted in Fig. 4. The corresponding IPRs indicate that $|\text{Vac}_\pm\rangle$ are localized state in the $\{|2l\rangle\}$ space. It is easy to check that the ground state of H_D within the region $\mu > \Delta$ is the vacuum state of two types of quasi-boson,

$$|G\rangle = |\text{Vac}_+\rangle |\text{Vac}_-\rangle, \quad (54)$$

with the groundstate energy $\varepsilon_+ + \varepsilon_- - \mu$, because the energy ε_\pm always positive.

(ii) In the region $\mu < \Delta$, we introduce another two independent boson operators

$$A_\rho = \sinh \frac{\varphi_\rho}{2} d_\rho^\dagger + \cosh \frac{\varphi_\rho}{2} d_\rho$$

where $\tanh(\varphi_\rho/2) = (\rho\Delta + \sqrt{-(\mu^2 + 2\rho\Delta\mu)}) / (\rho\Delta + \mu)$, to rewrite H_{eff} in the form

$$H_{\text{eff}} = \sum_{\rho=\pm} -\frac{1}{2} \sqrt{-(\mu^2 + 2\rho\Delta\mu)} (A_\rho^\dagger A_\rho^\dagger + A_\rho A_\rho), \quad (55)$$

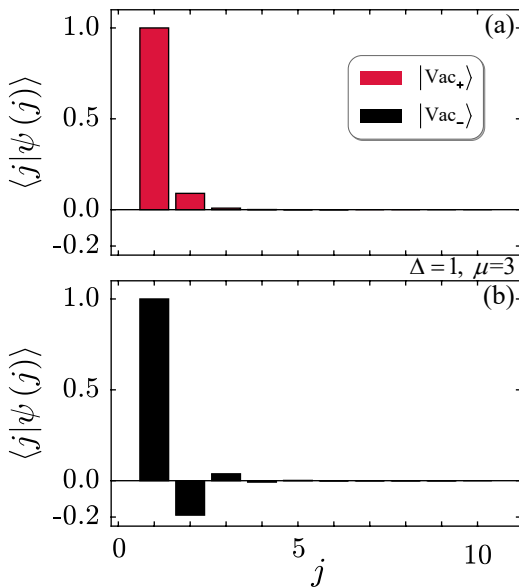


FIG. 4. Plots of two eigenstates of the effective model Eq. (41), specifically the vacuum state, as given by Eq. (50), with the system parameters $\Delta = 1$ and $\mu = 3$ for figures (a) and (b). In these plots, the red or black bars represent the real or imaginary parts of the amplitudes, respectively, and all are analytically determined.

which are exactly solvable based on the analysis in the last section.

A natural question arises: How can we detect the existence of the hidden EP in the Dicke model? Specifically, how can we identify the transition point between localized and extended phases experimentally? We begin with a dynamical method to differentiate between extended and localized regions. As shown in the last section, some localized eigenstates have a finite probability on the vacuum state $|0\rangle$ of the operator d_ρ . In contrast, nonlocalized eigenstates have an infinitesimal probability on the vacuum state of the operator d_ρ . This feature forms the foundation for the dynamical detection of the transition.

We consider the time evolution of an initial state $|0\rangle$. When $\mu > 2\Delta$, it represents a superposition of a set of localized eigenstates, while for $\mu < 2\Delta$, it represents nonlocalized eigenstates. In the former case, the profile of the evolved state remains stationary or does not spread. Conversely, in the latter case, the evolved state will move away or spread out. These differences should result in two distinct dynamic behaviors for the average number of photons in the Dicke model: it is finite when $\mu > 2\Delta$, while it explodes when $\mu < 2\Delta$.

The experimental scheme involves considering a quench process from the empty state $|0\rangle_p |\downarrow\rangle$, in which the photon number is zero and all N atoms are in the ground state, that is, $a|0\rangle_p = 0$ and $J_z |\downarrow\rangle = -N/2$. The numerical simulation is performed by computing the time evolution of an initial state $|\Psi(0)\rangle = |0\rangle_p |\downarrow\rangle$ under the

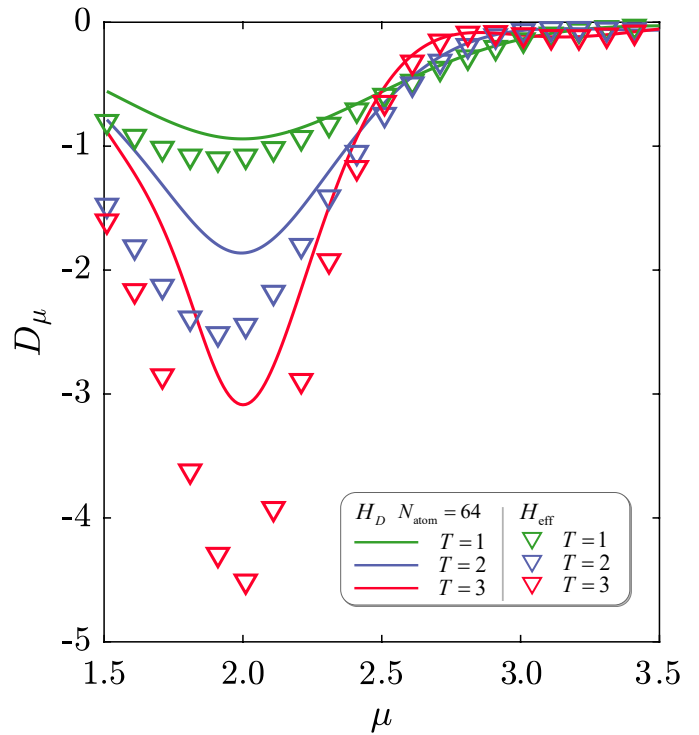


FIG. 5. Plots of D_μ , the derivative of the average photon number over a period of time T with respect to μ ($\Delta = 1$), as defined by Eq. (57). The numerical results are obtained through exact diagonalizations of the matrix representations for both the Dicke Hamiltonian Eq. (39) and the effective Hamiltonian Eq. (41), under the truncation of the photon number. The time interval T and the number of atoms N_{atom} are indicated in the panel. The results show that each D_μ has a minimum near the EP at $\mu = 2$. The valleys become deeper as T or N_{atom} increases, implying that D_μ is divergent at the EP in the case of infinite T and N_{atom} .

original Hamiltonian H_D given by the Eq. (39). We use the average number of photons for the evolved state $|\Psi(t)\rangle$, which is given by

$$N_P(t) = \langle \Psi(t) | a^\dagger a | \Psi(t) \rangle = \left| a e^{-iH_D t} |0\rangle_p |\downarrow\rangle \right|^2, \quad (56)$$

to measure the difference of the two phases separated by the EP. In order to detect the accurate transition point, we calculate the derivative of the the average photon number over a period of time T with respect to μ ,

$$D_\mu = \frac{\partial}{\partial \mu} \left[\frac{1}{T} \int_0^T N_P(t) dt \right]. \quad (57)$$

According to the analysis above, the average photon number should increase as T increases for $\mu < 2\Delta$, while it should remain a finite constant for $\mu > 2\Delta$. Then, at the EP, the average photon number should experience a jump, resulting in the divergence of D_μ in the limit as

$T \rightarrow \infty$. It is expected that D_μ has an extremum near the EP. The numerical results presented in Fig. 5 demonstrate a good match between the dynamic behavior and the transition point, indicating that our method is highly efficient.

VI. SUMMARY

In summary, we have revealed the possible connection between the QPT in a Hermitian system and the EP hidden within it, based on the solutions of the bosonic Kitaev model. As a candidate model to demonstrate the issue, such a model has two properties: (i) The degree of freedom in the bosonic Kitaev model is infinite, even for finite size system; (ii) The core matrix for its Nambu representation is non-Hermitian. In this sense, the EPs

is no longer a unique feature for non-Hermitian systems. Technically, we demonstrate the connection between the hidden EPs and the localization-delocalization transition in equivalent systems by mapping the Hamiltonian onto a set of equivalent single-particle systems using a BCS-like pairing basis. We also propose a scheme for the experimental detection of the transition in a Dicke model, based on the measurement of the average number of photons for the quench dynamics starting from the empty state. Our work may open a new research area for uncovering the hidden EPs in a Hermitian system that govern the QPTs.

ACKNOWLEDGMENT

We acknowledge the support of NSFC (Grants No. 12374461).

-
- [1] Tosio Kato. *Perturbation theory for linear operators*, volume 132. Springer Science & Business Media, 2013.
 - [2] Michael V Berry. Physics of nonhermitian degeneracies. *Czechoslovak journal of physics*, 54(10):1039–1047, 2004.
 - [3] Walter D Heiss. The physics of exceptional points. *Journal of Physics A: Mathematical and Theoretical*, 45(44):444016, 2012.
 - [4] XM Yang, XZ Zhang, C Li, and Z Song. Dynamical signature of the moiré pattern in a non-hermitian ladder. *Phys. Rev. B*, 98(8):085306, 2018.
 - [5] KL Zhang and Z Song. Resonant-amplified and invisible bragg scattering based on spin coalescing modes. *Phys. Rev. B*, 102(10):104309, 2020.
 - [6] KL Zhang, L Jin, and Z Song. Helical resonant transport and purified amplification at an exceptional point. *Phys. Rev. B*, 100(14):144301, 2019.
 - [7] Jörg Doppler, Alexei A. Mailybaev, Julian Böhm, Ulrich Kuhl, Adrian Girschik, Florian Libisch, Thomas J. Milburn, Peter Rabl, Nimrod Moiseyev, and Stefan Rotter. Dynamically encircling an exceptional point for asymmetric mode switching. *Nature*, 537(7618):76–79, September 2016.
 - [8] H. Xu, D. Mason, Luyao Jiang, and J. G. E. Harris. Topological energy transfer in an optomechanical system with exceptional points. *Nature*, 537(7618):80–83, September 2016.
 - [9] Sid Assaworarith, Xiaofang Yu, and Shanhui Fan. Robust wireless power transfer using a nonlinear parity-time-symmetric circuit. *Nature*, 546(7658):387–390, June 2017.
 - [10] Jan Wiersig. Enhancing the sensitivity of frequency and energy splitting detection by using exceptional points: Application to microcavity sensors for single-particle detection. *Phys. Rev. L*, 112:203901, May 2014.
 - [11] Jan Wiersig. Sensors operating at exceptional points: General theory. *Phys. Rev. A*, 93:033809, Mar 2016.
 - [12] Hossein Hodaei, Absar U. Hassan, Steffen Wittek, Hipolito Garcia-Gracia, Ramy El-Ganainy, Demetrios N. Christodoulides, and Mercedeh Khajavikhan. Enhanced sensitivity at higher-order exceptional points. *Nature*, 548(7666):187–191, August 2017.
 - [13] Weijian Chen, Şahin Kaya Özdemir, Guangming Zhao, Jan Wiersig, and Lan Yang. Exceptional points enhance sensing in an optical microcavity. *Nature*, 548(7666):192–196, August 2017.
 - [14] L Jin and Z Song. Physics counterpart of the pt non-hermitian tight-binding chain. *Phys. Rev. A*, 81(3):032109, 2010.
 - [15] L Jin and Z Song. Partitioning technique for discrete quantum systems. *Phys. Rev. A*, 83(6):062118, 2011.
 - [16] L Jin and Z Song. A physical interpretation for the non-hermitian hamiltonian. *Phys. Rev. A*, 44(37):375304, 2011.
 - [17] XZ Zhang, L Jin, and Z Song. Self-sustained emission in semi-infinite non-hermitian systems at the exceptional point. *Phys. Rev. A*, 87(4):042118, 2013.
 - [18] Alexander McDonald, T Pereg-Barnea, and AA Clerk. Phase-dependent chiral transport and effective non-hermitian dynamics in a bosonic kitaev-majorana chain. *Phys. Rev. X*, 8(4):041031, 2018.
 - [19] Yu-Xin Wang and AA Clerk. Non-hermitian dynamics without dissipation in quantum systems. *Phys. Rev. A*, 99(6):063834, 2019.
 - [20] Vincent P Flynn, Emilio Cobanera, and Lorenza Viola. Deconstructing effective non-hermitian dynamics in quadratic bosonic hamiltonians. *New Journal of Physics*, 22(8):083004, 2020.
 - [21] Javier Del Pino, Jesse J Slim, and Ewold Verhagen. Non-hermitian chiral phononics through optomechanically induced squeezing. *Nature*, 606(7912):82–87, 2022.
 - [22] Ya-Nan Wang, Wen-Long You, and Gaoyong Sun. Quantum criticality in interacting bosonic kitaev-hubbard models. *Phys. Rev. A*, 106(5):053315, 2022.
 - [23] Thomas Bilitewski and Ana Maria Rey. Manipulating growth and propagation of correlations in dipolar multilayers: From pair production to bosonic kitaev models. *Phys. Rev. L*, 131(5):053001, 2023.
 - [24] Mariam Ughrelidze, Vincent P Flynn, Emilio Cobanera, and Lorenza Viola. Interplay of finite-and infinite-size stability in quadratic bosonic lindbladians. *Phys. Rev. A*, 110(3):032207, 2024.

- [25] Jesse J Slim, Clara C Wanjura, Matteo Brunelli, Javier Del Pino, Andreas Nunnenkamp, and Ewold Verhagen. Optomechanical realization of the bosonic kitaev chain. *Nature*, 627(8005):767–771, 2024.
- [26] Jamal H Busnaina, Zheng Shi, Alexander McDonald, Dmytro Dubyna, Ibrahim Nsanzineza, Jimmy SC Hung, CW Sandbo Chang, Aashish A Clerk, and Christopher M Wilson. Quantum simulation of the bosonic kitaev chain. *Nature Communications*, 15(1):3065, 2024.
- [27] Jia-Ming Hu, Bo Wang, and Ze-Liang Xiang. Bosonic holes in quadratic bosonic systems. *arXiv preprint arXiv:2408.01059*, 2024.
- [28] A Yu Kitaev. Unpaired majorana fermions in quantum wires. *Physics-uspekhi*, 44(10S):131, 2001.